

The Universality Class of Diffusion Limited Aggregation and Viscous Fingering

Joachim Mathiesen,¹ Itamar Procaccia,² Harry L. Swinney,³ and Matthew Thrasher³¹NTNU, Institutt for Fysikk, 7491 Trondheim, Norway²The Department of Chemical Physics, The Weizmann Institute of Science, Rehovot 76100, Israel³Center for Nonlinear Dynamics and Department of Physics, University of Texas at Austin, Texas 78712

We investigate whether fractal viscous fingering and diffusion limited aggregates are in the same scaling universality class. We bring together the largest available viscous fingering patterns and a novel technique for obtaining the conformal map from the unit circle to an arbitrary singly connected domain in two dimensions. These two Laplacian fractals appear different to the eye; in addition, viscous fingering is grown in parallel and the aggregates by a serial algorithm. Nevertheless, the data strongly indicate that these two fractal growth patterns are in the same universality class.

Laplacian fractals are paradigmatic examples for the spontaneous growth of fractal patterns in natural systems. In particular, two such examples have attracted an enormous amount of interest: viscous fingering and diffusion limited aggregation (DLA).

Viscous fingering is realized [1] when a less viscous fluid displaces a more viscous fluid contained in the narrow gap between two glass plates (a Hele-Shaw cell). When the less viscous fluid is inserted through an aperture in one of the glass plates, a pattern is formed, as shown in Fig. 1 [2]. The fluid velocity v of the displaced fluid in a Hele-Shaw cell satisfies Darcy's law, $v \propto r/p$, where p is the pressure. To a very good approximation, the viscous fluid is incompressible (i.e., $\nabla \cdot v = 0$), so the pressure in the viscous fluid satisfies the Laplace equation $\nabla^2 p = 0$.

DLA is realized [3] as a computer experiment in which a fractal cluster is grown by releasing a fixed size random walker from infinity, allowing it to walk until it hits any particle already belonging to the cluster. Since the particles are released one by one and may take a long time to hit the cluster, the probability field is stationary and, in the complement of the cluster, we have again $\nabla^2 p = 0$.

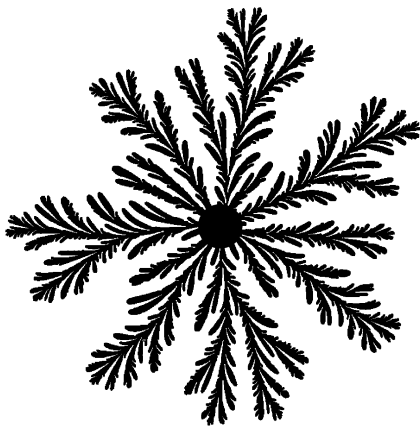


FIG. 1: Digitized image of an experimental viscous fingering pattern. A fluid (black) is injected into the oil-filled gap (white). The pattern is approximately 22 cm in diameter, cf. [2].

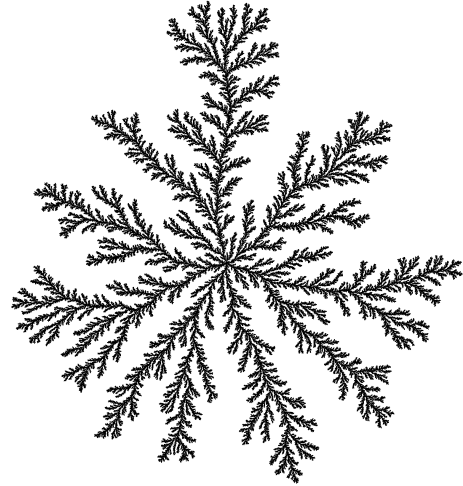


FIG. 2: A diffusion limited aggregate with 50,000,000 particles. Image courtesy of Elak Somfai.

A typical DLA cluster is shown in Fig. 2.

Mathematically, these problems are similar but not identical. In both cases, one solves the Laplace equation with the same boundary condition at infinity, i.e. $\nabla p = \text{const} \hat{r}$ as $r \rightarrow \infty$. However, in viscous fingering, each point on the fractal's boundary advances at a rate proportional to r/p , whereas the DLA accretes one particle at a time, changing the Laplacian field after each such growth step. Thus, we refer to viscous fingering and DLA as parallel and serial processes, respectively. In addition, the ultraviolet regularization differs; in DLA, $p = 0$ on the cluster and the regularization is provided by the particle size. In viscous fingering, one solves the problem with the boundary condition $p = \gamma/\kappa$ where γ is the surface tension and κ is the local curvature. Finally, viscous fingers are grown in a finite gap and are not truly 2-dimensional. Accordingly, one can ask whether these two fractal growth problems are in the same scaling universality class. But to answer this question, one must first define what one means by a "scaling universality class."

Definition of the scaling universality class: The first test of correspondence between the fractal patterns

has to do with their fractal dimension D_0 . Denote by R_n the radius of the minimal circle that contains a fractal pattern. The fractal dimension is defined by how the mass M_n contained within this circle (number of particles for DLA, area for viscous fingers) scales with R_n , $M_n \propto R_n^{D_0}$. Measurements of this type indicated a value $D_0 \approx 1.71$ for both problems, motivating many authors to express the opinion that these two problems are in the same universality class [2, 4]. Obviously, the fractal dimension by itself is not sufficient, and a more stringent definition is necessary.

We propose here that the identity of the scaling properties of the harmonic measure is a sufficient test for two Laplacian growth problems to be in the same universality class. The harmonic measure is the probability for a random walker to hit the boundary of the fractal pattern. It determines the growth in both problems, being proportional to r^q at the boundary. Suppose that we know the probability measure $\rho(s)ds$ for a random walker to hit an infinitesimal arc length on the fractal boundary. We compute the probability $P_i(q)$ that the i th box $\rho(s)ds$, and then define the generalized dimensions [5] via

$$D_q = \lim_{N \rightarrow \infty} \frac{\log \sum_{i=1}^N P_i(q)}{(q-1) \log N}; \quad (1)$$

where $N(q)$ is the number of boxes of size ϵ that cover the fractal boundary. The $q > 0$ branch of this function probes the high probability region of the measure, whereas the $q < 0$ branch stresses the low probabilities. For $q \rightarrow 0^+$ we find the fractal dimension D_0 . An equivalently useful description [6] is provided by the scaling indices that determine how the measure becomes singular, $P_i(q) \propto \epsilon^{f(q)}$, as $\epsilon \rightarrow 0$. This set of indices is accompanied by $f(q)$ which is the fractal dimension of the subset of singularities of scaling exponent q . The relation of these objects to D_q is in the form of the Legendre transform

$$f(q) = \frac{\partial [(q-1)D_q]}{\partial q}; \quad (2)$$

$$f(q) = q D_q - (q-1)D_q. \quad (3)$$

In fractal measures defined on simple fractals, the values of $f(q)$ are usually bounded from above and from below, $f_{\min} \leq f(q) \leq f_{\max}$. When the fractal measure fails to exhibit power law scaling everywhere (say, $P_i(q) \propto \epsilon^{f(q)}$ somewhere), one finds a phase transition in this formalism [7] with one of the edge values f_{\min} or f_{\max} ceasing to exist. When the spectrum of exponents $f(q)$ and their frequency of occurrence $f(q)$ in two problems are the same, we refer to these problems as being in the same universality class. We note that a similar criterion was used to state that different dynamical systems are in the same universality class at their transition to chaos [8], but not many other physical problems yielded to such a stringent test, simply because it is not easy to compute with enough precision the scaling properties of fractal measures. For DLA, such an accurate computation was

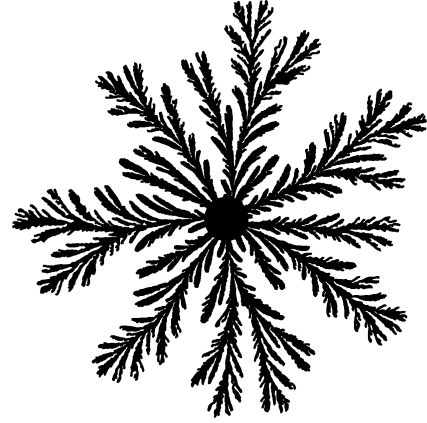


FIG. 3: Conformal map of the unit circle aimed to fit the pattern in Fig. 1. The map was constructed using the algorithm proposed in the text, transforming the unit disc represented by the black area. This figure demonstrates the accuracy of our method for reproducing complex patterns.

achieved [9]; in this Letter, we report also an accurate computation for experimental viscous fingering patterns, allowing us to test whether the two problems are in the same universality class.

The apparent complexity of the viscous fingers is discouraging for any attempt to calculate the harmonic measure reliably. The naive method for computing the harmonic measure for DLA is to "probe" the interface with random walkers and perform frequency statistics [10]. While the statistics at the outer tips is reasonable [11], the deep fjords are visited extremely rarely by the random walkers. Similarly, in viscous fingering experiments, the measure is usually estimated from the velocity of the interface [12]. Obviously, this reveals the outer tips which move with an appreciable velocity, but leaves unmeasured the harmonic measure on the fjords, which almost do not move at all. One has to look for alternative methods.

The harmonic measure from iterated conformal maps: The Riemann theorem guarantees that there exists a conformal map from the exterior of the unit circle $|z| = 1$ to the exterior of our viscous fingering patterns. Having such a conformal map, say $w = \phi(z)$, the harmonic measure is simply obtained as $1 = \int_0^1 \rho(w) |dw|$ up to normalization. The actual construction of such a map for a given well-developed fractal pattern is, however, far from obvious, and it has never been accomplished before. We will demonstrate now that the method of iterated conformal maps [13, 14] can be adapted to solve this problem in a very efficient way. We use data acquired in experiments, in which air is injected into oil from a central orifice. The oil is confined between two circular glass plates, 288 mm in diameter and each 60 mm thick [2]. The plates are separated by 0.127 mm and are flat to 0.13 μ m (optically polished to one-quarter of a wavelength). An oil bubble surrounds the plates. The data presented here were obtained with silicone oil with a dynamic viscosity $\eta = 345$

mPa s and surface tension $\gamma = 20.9 \text{ mN/m}$ at 24°C ; additional experiments were conducted with silicone oil with a dynamic viscosity $\eta = 50.8 \text{ mPa s}$ and surface tension $\gamma = 20.6 \text{ mN/m}$ at 24°C . The pressure difference Δp between the injected air and the oil buffer ranged from 0.1 to 1.25 atm. The 1 mm diameter central hole through which the air is injected cannot be seen in Fig. 1, rather the 22 mm diameter central solid circular region (black) is a mask introduced after the images have been digitized. The interface near the injection point could not be extracted because of light contrast limitations.

The images are digitized and each pixel is given an index j from 1 to N . As a first step, we rescale all the pixels and apply a uniform shift such that the central black region becomes the unit circle. Next, we record the position of each pixel in the complex plane, denoting it by $z_j = x_j + iy_j$. Next, we sort the pixels in ascending order with respect to $|z_j|$, which is the minimal distance r_j of the j 'th pixel from the interface of the fractal pattern. We divide the sorted pixels into m groups, such that the k 'th group contains the pixels which have absolute values smaller than those in the $(k+1)$ 'th group. Within the individual groups, we once again divide the pixels into two subgroups, where the first subgroup contains the pixels with associated radii r_j larger than a threshold value ϵ . Typically, we choose ϵ to be $\sqrt{2}$ times the pixel size. We build the conformal mapping from the unit circle to the viscous fingers by expanding stepwise the unit circle in the interior part of the viscous fingers. The size of the expansion is given by r_j . In other words, in the n 'th step we build a conformal mapping $w^{(n)}(z)$ from the z complex plane to the w complex plane. At each step, we employ an auxiliary mapping f , that locally perturbs the unit circle with a semicircular bump centered at the position $e^{i\alpha}$ and of linear size ϵ . The construction is done such that we first expand around the points in the first subgroup of the first group, then we proceed to the second subgroup. Once we have finished expanding around the first group, we move on to the second group, etc. Most pixels in the vicinity of the pixel z_j will be covered when expanding the conformal mapping around z_j ; therefore, they can be disregarded in all future iterations. In fact, a majority of the pixels will be covered by expansions around nearby points. Thus we need to perform a significantly smaller number of expansions than the number of pixels. The aforementioned division of the pixels is a simple way to speed up our method, i.e. to reduce the number of necessary expansions. We first expand the mapping around the points $w^{(n)}(z_j)$ with large radii ($r_j > \epsilon$) and close to the unit circle. The conformal mapping is constructed by successive iterations. In each iteration step, the mapping covers more and more of the viscous fingers, and the number of pixels not being covered decreases.

Assume that we have reached the n 'th iteration step. Considering the pixels that are not covered, we now use the inverse mapping, $z^{(n)} = w^{(n)-1}$, to map these pixels z_j to the exterior of the unit circle, i.e. we map them from the z -plane to the w -plane. The size ϵ_{n+1} of the

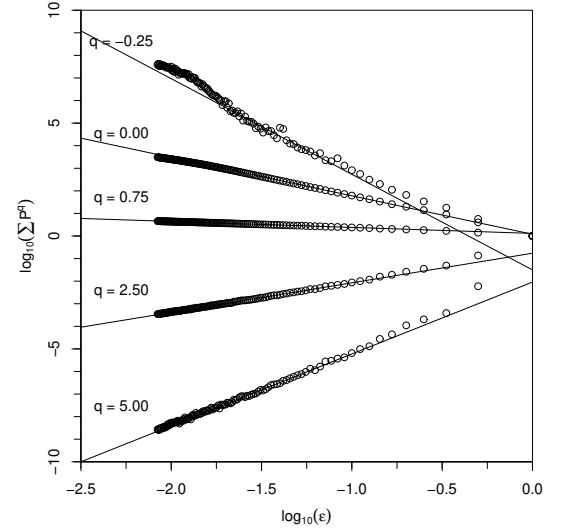


FIG. 4: Log-log plots of $\prod_{i=1}^N P_i^q(\epsilon)$ vs. the box size ϵ for selected values of q . We find reliable power law scaling for $q \geq 0.25$.

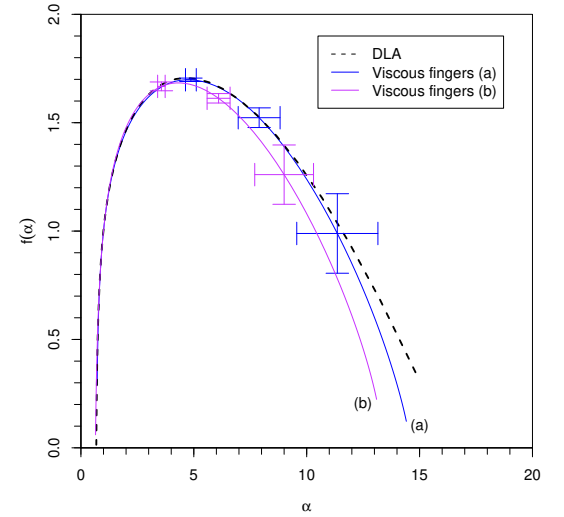


FIG. 5: $f(\alpha)$ curves for the harmonic measure of the experimental viscous fingers patterns and its comparison with the $f(\alpha)$ curve of the harmonic measure of DLA. (a) is averaged over 15 patterns obtained with a silicone oil with a dynamic viscosity $\eta = 345 \text{ mPa s}$ and (b) is averaged over 15 patterns with $\eta = 50.8 \text{ mPa s}$.

$(n+1)$ 'th bump to be centered at the position z_j is taken to be

$$\epsilon_{n+1} = \frac{r_j}{\epsilon^{(n)}(e^{i\alpha_{n+1}})}; \text{ where } \alpha_{n+1} = \arg w^{(n)}(z_j); \quad (4)$$

From the unit circle, we now advance along the shape by expanding around the next z_j , according to the scheme described above.

The efficiency of this method is surprising; the number

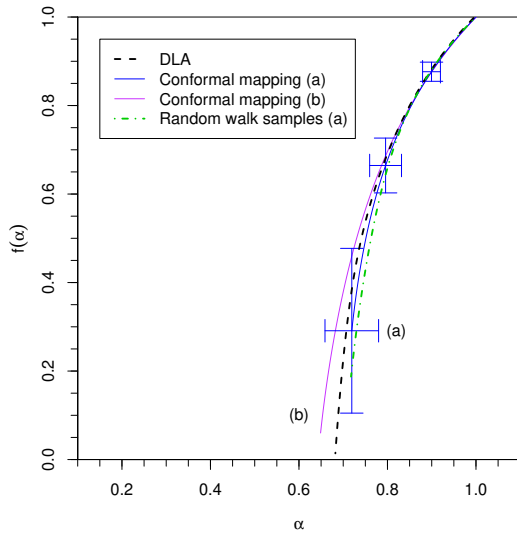


FIG. 6: Close-up of the $f(\alpha)$ curves presented in Fig. 5 together with the same curve computed from a sampling with random walkers.

of iterations needed to build the conformal map remains rather low even for a complex pattern like that in Fig. 1. Figure 3 presents the result of our method using the digitalized image of viscous fingers shown in Fig. 1. Indeed, the conformal map accurately reproduces the image. In general, the number of iterations is around 10000-20000 for the maps that we analyze in this Letter.

Results: With the conformal mapping at hand, we have the harmonic measure as $1 = \sum_{j=0}^{(n)} j$. One has to be cautious in evaluating the derivative, since inside the fjords, the measure becomes so small that it is difficult to resolve the fjords on the unit circle. The way to evaluate the derivative involves a careful book keeping of the positions of the individual bumps added in each iteration step [14]. In Fig. 4 we present log-log plots of the sum

$P_{i=1}^N(\alpha) P_i^q(\alpha)$ vs. the box size α for selected values of q . The estimated slopes, $(q) = (q-1)D_q$, are very reliable for positive values of q . As seen in Fig. 4, for values of $q < 0.25$, the power-law scaling is lost. In DLA, the deep fjords become dominant for $q < 0.2$, and lead to a nonanalyticity in the $f(\alpha)$ curve, a phenomenon known as a "phase transition" in the thermodynamic formalism of the fractal measure [7].

We can now use the measured values of (q) to extract the $f(\alpha)$ curve. The result is shown in Fig. 5 together with the same curve for the harmonic measure of DLA. While there is no alternative way to compute this function in its entirety, we can test the accuracy of our results by looking at $f(\alpha)$ for $q > 1$, which characterizes the highly probable regions of harmonic measure near the tips. We sampled the tips of the experimental data with random walkers, a good method as long as one studies the part of the multifractal spectrum for $q > 1$. For the sampling, we use 10^6 random walkers. Increasing this number did not lead to a significant change in the results. Figure 6 shows a close-up of the $f(\alpha)$ curve presented in Fig. 5, alongside the one computed from the random walk samples. There is almost no difference in the left hand branches, and we thus conclude that our method is fully adequate for representing the tips of the viscous fingers. The estimate of m_{in} is the same (within the uncertainty of 0.06) as the one computed for DLA, which was $m_{in} = 0.67$ [15].

In conclusion, we have presented a powerful method for the construction of a conformal map from the unit circle to complex fractal patterns. Using this conformal map, we can compute accurately the fractal measure and determine its scaling properties. The comparisons shown in Figs. 5 and 6 strongly indicate that viscous fingering and DLA are in the same universality class within the experimental uncertainty. Future study can determine whether this correspondence extends to the nonanalyticity in the $f(\alpha)$ curve.

[1] G. Daccord, J. Nittman, and H.E. Stanley, Phys. Rev. Lett. 56, 336 (1986).
[2] O. Praud and H.L. Swinney, Phys. Rev. E 72, 011406 (2005).
[3] T.A. Witten and L.M. Sander, Phys. Rev. Lett. 47, 1400 (1981).
[4] See for example, L. Paterson, Phys. Rev. Lett. 52, 1621 (1984), L.M. Sander, Nature (London) 322, 789 (1986), J. Nittman and H.E. Stanley, Nature 321, 663 (1986).
[5] H.G.E. Hentschel and I. Procaccia, Physica D 8, 435 (1983).
[6] T.C. Halsey, M.H. Jensen, L.P. Kadano, I. Procaccia, and B. Shraiman, Phys. Rev. A 33, 1141 (1986).
[7] D. Katzen and I. Procaccia, Phys. Rev. Lett. 58, 1169 (1987).
[8] M.H. Jensen, A. Libchaber, L.P. Kadano, I. Procaccia, and J. Stavans, Phys. Rev. Lett. 55, 2798 (1985).

[9] B. Davidovitch, M.H. Jensen, A. Levermann, J. Mathiesen, and I. Procaccia, Phys. Rev. Lett. 87, 164101 (2001).
[10] C. Amitrano, A. Coniglio, and F. diLiberto, Phys. Rev. Lett. 57, 1016 (1986).
[11] T.C. Halsey, P. Meakin, and I. Procaccia, Phys. Rev. Lett. 56, 854 (1986).
[12] K.J. Malby, F. Boger, J. Feder, and T. Jossang, in Time Dependent Effects in Disordered Materials, edited by R. Pynn and T. Riste (Plenum, New York, 1987), p.111.
[13] M.B. Hastings and L.S. Levitov, Physica D 116, 244 (1998).
[14] M.H. Jensen, A. Levermann, J. Mathiesen, and I. Procaccia, Phys. Rev. E 65, 046109 (2002).
[15] M.H. Jensen, J. Mathiesen, and I. Procaccia, Phys. Rev. E 67, 042402 (2003).